Supporting Information

Low-temperature Li-S Battery Enabled by CoFe bimetallic Catalysts

Ning Gao[a], Yujiao Zhang[a], Chong Chen[b], Bao Li[c], Wenbiao Li[a], Huiqiang Lu[d], Le Yu[b]*, Shumin Zheng[a]*, and Bao Wang[a]*

[a]*State Key Laboratory of Biochemical Engineering, Institute of Process Engineering, Chinese Academy of Sciences, Beijing, 100190, P. R. China. E-mail: smzheng@ipe.ac.cn; baowang@ipe.ac.cn*

[b]*State Key Lab of Organic-Inorganic Composites, Beijing Advanced Innovation Center for Soft Matter Science and Engineering, Beijing University of Chemical Technology, Beijing, 100029, P. R. China. E-mail: yule@mail.buct.edu.cn*

[c]*School of Chemistry and Chemical Engineering, Henan Normal University, Xinxiang, 453007, P. R. China*

[d]*Ganzhou Key Laboratory for Drug Screening and Discovery, School of Geography and Environmental Engineering, Gannan Normal University, Ganzhou, 341000, P. R. China*

Experimental Section

Synthesis of CoFe@C@CNFs

The impregnation method, a classic method for preparing heterogeneous catalysts, was used to synthesize the target product. $CoCl_2 \cdot 6H_2O$ and $FeCl_3 \cdot 6H_2O$ with the same amount of substance were evenly mixed in 30mL deionized water, to obtain a Co^{2+}/Fe^{3+} metal salt mixed solution. The pre-cut trans blot filter paper (denoted as BP) was soaked in the mixed solution for 2 h. The size of the BP was calculated according to the actual shrinkage rate and cut into the disk shape required by the cathode electrode. Then, the BP adsorbed metal ions were dried at 60 °C for 12 h. Finally, the dried BP was calcined for 2 h in the Ar/H_2 atmosphere at 800 °C to prepare the CoFe@C@CNFs. In this work, we adopted metal ion concentrations of 20, 40, and 80 mM, respectively. We marked the prepared samples in different proportions as CoFe@C@CNFs-20, CoFe@C@CNFs-40, and CoFe@C@CNFs-80. For comparison, the synthesis of CNFs was the same as above, but $CoCl_2 \cdot 6H_2O$ and $FeCl_3 \cdot 6H_2O$ were not added to the deionized water.

Preparation and Visualized Adsorption Test of Li_2S_6

The sublimated sulfur and Li_2S (molar ratio = 5:1) were dissolved in 1,3-dioxolane/1,2-dimethoxyethane (DOL/DME, volume ratio was 1:1), to prepare the Li_2S_6 solution (1 M, molar concentration calculated according to sulfur atoms). The mixture was stirred at 60 °C for 48 h, and the whole process was carried out in an Ar-filled glovebox. Then, 10 mg of samples (CNFs or CoFe@C@CNFs) were placed in the 3 mL of the diluted Li_2S_6 solutions (5 mM) for 3 h.

Characterization

The morphologies and structures of the prepared samples were characterized with Zeiss Supra55 Scanning Electron Microscopy (SEM) and FEI TECNAIG2 F30 Transmission Electron Microscopy (TEM). X-ray diffraction (XRD) measurements were performed using Rigaku D/max 2550 PC (CuKa). Raman spectra were recorded by a Renishaw Raman spectroscope under 532 nm laser excitation. Brunauer Emmett Teller (BET) surface area

measurements were measured by nitrogen adsorption and desorption method using an ASAP 2020 Analyser. The accurate elemental composition and valence state were determined by X-ray photoelectron spectroscopy (XPS) were collected at an Escalab 250Xi spectrophotometer. Thermogravimetric (TG) analysis was recorded by a TG-209F1 under air atmosphere with a heating rate of 5°C min^{-1}.

Cell Assembly and Electrochemical Measurements

The Li_2S_6 catholyte was added to the synthesized cathode to form Li_2S_6/CoFe@C@CNFs composite electrode. The S loading is 1 mg cm^{-2}, corresponding to 26 μL of 0.2 M Li_2S_6. The electrolyte was 1.0 M bis-(trifluoromethane) sulfonamide lithium (LiTFSI) in DOL/DME (volume ratio = 1:1) with 0.2 M $LiNO_3$, 50 μL electrolyte was used in each cell. CR2032 coin cells were assembled using the Li_2S_6/CoFe@C@CNFs cathode, lithium metal anode, and Celgard 2300 separator. Galvanostatic discharge/charge tests were recorded on the Neware battery test system between 1.7 and 2.8 V (*vs*. Li/Li^+). The cyclic voltammetry (CV) and electrochemical impedance spectroscopy (EIS) were conducted by a bio-logic VMP3 electrochemical workstation.

Assembly and Measurement of Symmetrical Cells

Li_2S_6 (0.5 M) provides the active substance and two same electrodes (CNFs or CoFe@C@CNFs) were served as the working and counter electrodes for the cell assembly. The electrode area was around 1 cm^{-2}. The assembled symmetric cells were tested by CV at a scan rate of 20 mV s^{-1} (potential window -0.8-0.8 V).

Theoretical computations

All DFT calculations were performed using the CP2K package,[1,2] employing a mixed scheme of plane waves and Gaussian-type basis sets. Plane waves with a cutoff of 420 Ry were used to calculate the charge density. The Kohn-Sham orbitals were expanded in Gaussian basis sets with triple-zeta plus polarization quality. The Goedecker pseudopotentials and the Perdew-Burke-Ernzerhof (PBE) functional were used.[3,4] The climbing nudged elastic band (CI-NEB)

method[5] was applied to search the transition states (TS) of elementary reaction. In each CI-NEB pathway, 8 images with starting and ending points were used to locate a saddle point on the potential energy surface.

The calculation of the adsorption energy was carried out by the following formula:[6]

$$E_{bind} = E_{total} - E_{Li2Sx} - E_{host}$$

Where E_{bind}, E_{total}, E_{Li2Sx}, and E_{host} are the adsorption energy value of the system, the total energy of the model, energy of Li_2S_x, and the energy of the surface model, respectively.

Gibbs free energy is the nature of the reaction system, the function of status, and is only determined by the beginning and end states of the system. The reaction of each step can be written as following equations:

$$*S_8 + 2Li^+ + 2e^- \rightarrow *Li_2S_8 \quad (S1)$$

$$3/2*Li_2S_8 + Li^+ + e^- \rightarrow 2*Li_2S_6 \quad (S2)$$

$$*Li_2S_6 + Li^+ + e^- \rightarrow 3/2*Li_2S_4 \quad (S3)$$

$$1/2*Li_2S_4 + Li^+ + e^- \rightarrow *Li_2S_2 \quad (S4)$$

$$1/2*Li_2S_2 + Li^+ + e^- \rightarrow *Li_2S \quad (S5)$$

The Gibbs free energies for all of the reaction steps as following equations:

$$\Delta G_1 = G(*Li_2S_8) - G(*S_8) - 2G(Li) \quad (S6)$$

$$\Delta G_2 = G(*Li_2S_6) + 2G(S) - 2G(*Li_2S_8) \quad (S7)$$

$$\Delta G_3 = G(*Li_2S_4) + 2G(S) - 2G(*Li_2S_6) \quad (S8)$$

$$\Delta G_4 = G(*Li_2S_2) + 2G(S) - 2G(*Li_2S_4) \quad (S9)$$

$$\Delta G_5 = G(*Li_2S) + G(S) - 2G(*Li_2S_2) \quad (S10)$$

For the DFT calculation of adsorbate, $G = H\text{-}TS = E_{DFT} + ZPE\text{-}TS$, where ZPE is zero-point energy and TS is the enthalpic temperature correction. The largest delta G will determine the overall speed of the Li-S battery reaction, and the corresponding reaction step is called the rate-

determining step.[6]

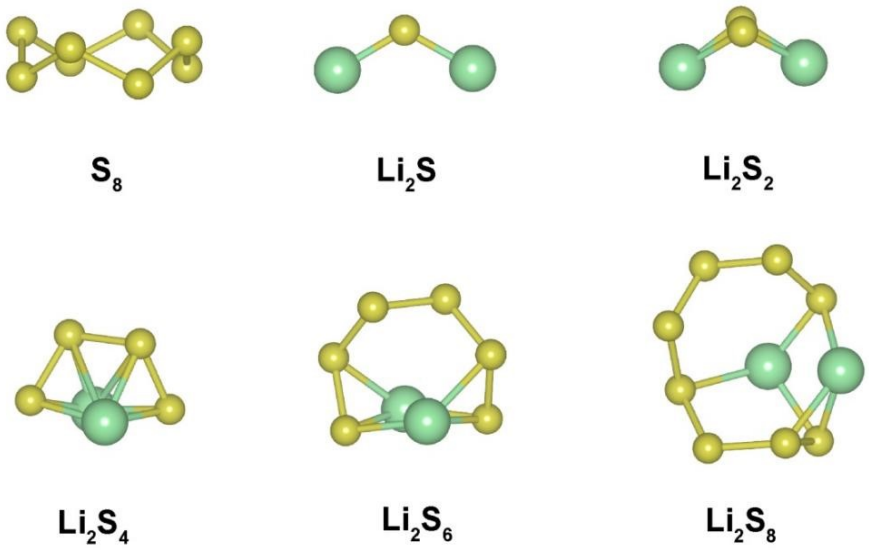

Fig. S1 Optimized configurations of sulfur, polysulfides, and disulfide.

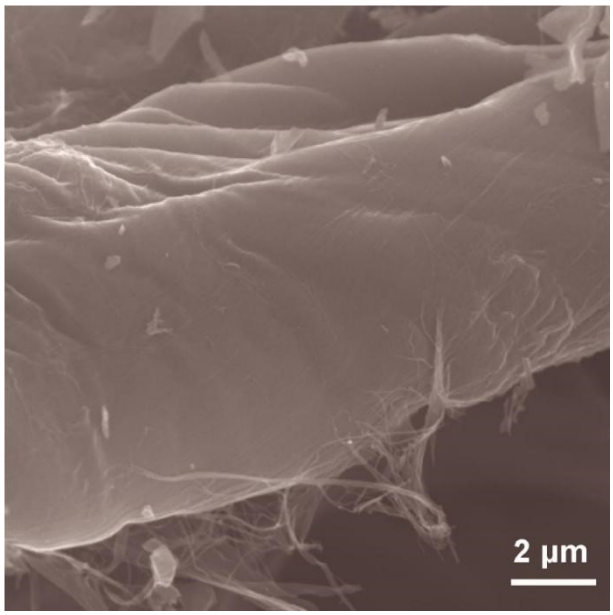

Fig. S2 Transverse SEM image of CoFe@C@CNFs.

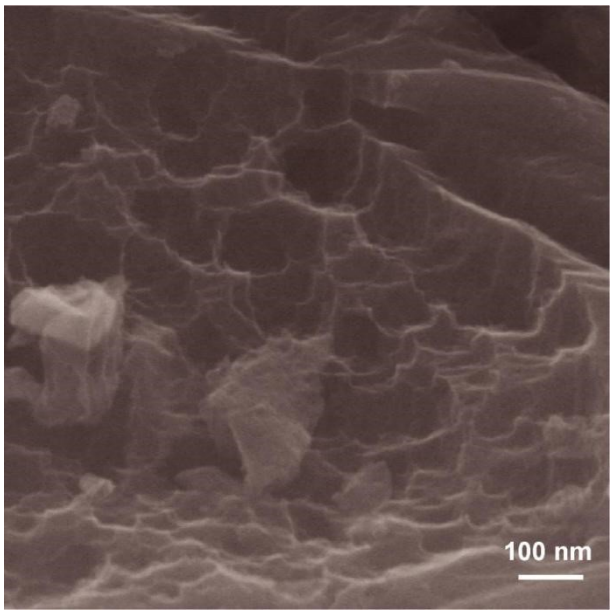

Fig. S3 Longitudinal SEM image of CoFe@C@CNFs.

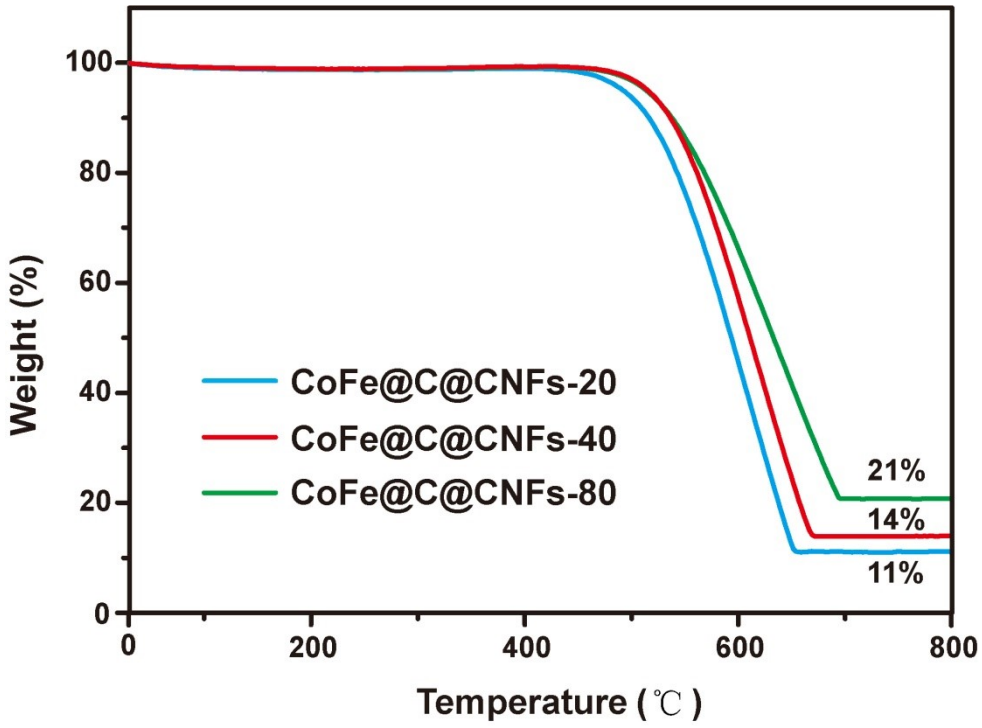

Fig. S4. TG data of composite materials with different metal concentrations.

During the thermogravimetric test, the Co-Fe particles in the CoFe@C@CNFs react with oxygen to form Co_3O_4 and Fe_2O_3. The contents of the two metals can be estimated by the following conservation of mass (Take CoFe@C@CNFs-20 as an example):

	$3\,Co \sim Co_3O_4$	;	$2\,Fe \sim Fe_2O_3$	
Molar mass:	177	241	112	160
Weight ratio:	59a	b	56a	11%-b
$\Longrightarrow$	Co : 59a = 4.05%	;	Fe : 56a = 3.84%	

Similarly, the content of other materials is shown in Table S1.

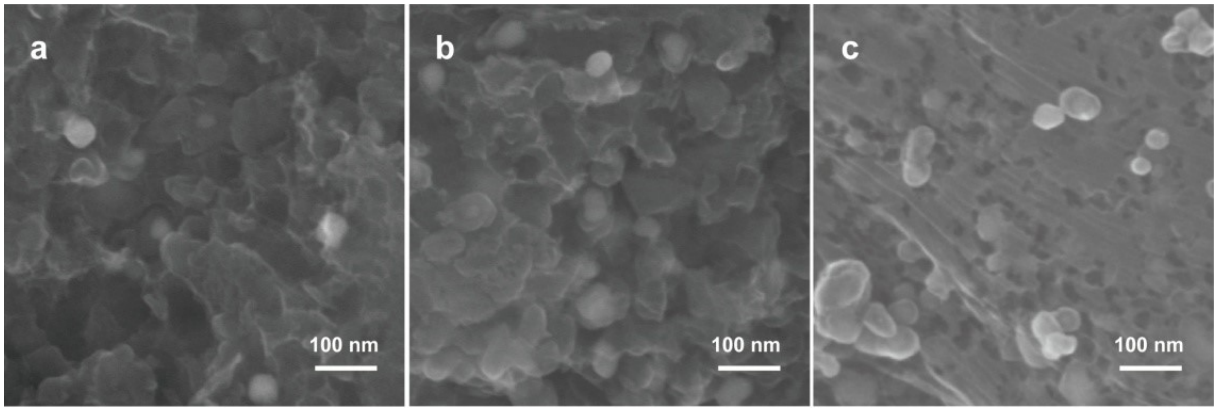

Fig. S5. SEM images of (a) CoFe@C@CNFs-20, (b) CoFe@C@CNFs-40 and (c) CoFe@C@CNFs-80.

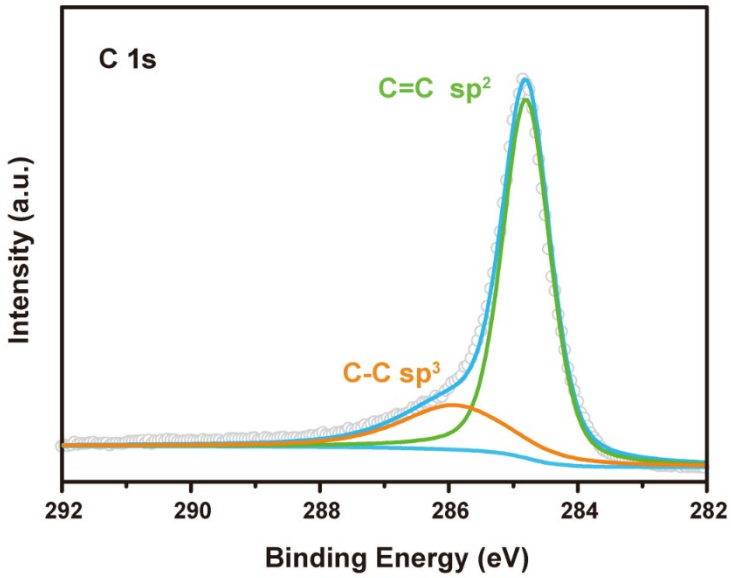

Fig. S6 C 1s XPS spectrum of CoFe@C@CNFs.

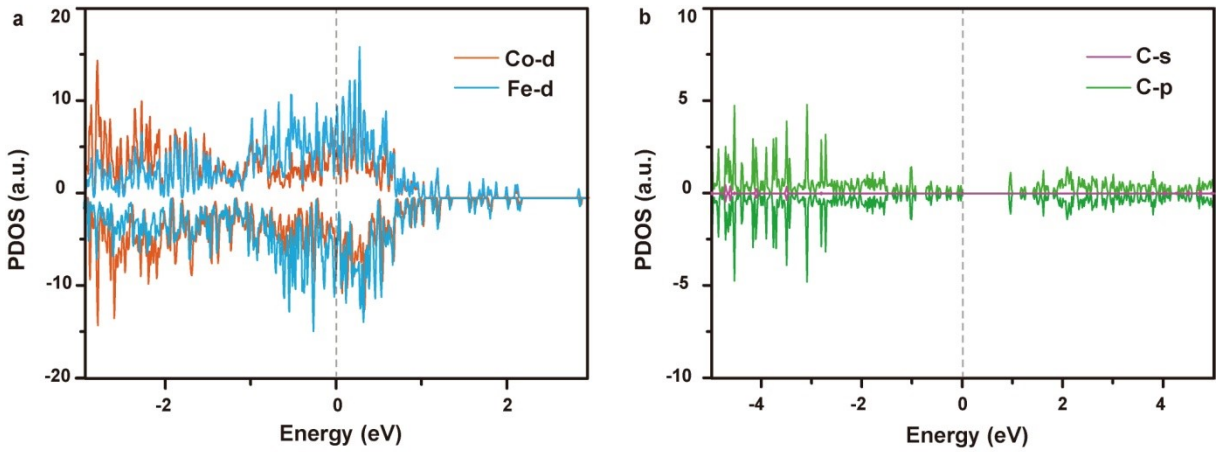

Fig. S7 Calculated spin-polarized DOS of the (a) CoFe surface and the (b) CNFs surface structure by using PBE functional. Dashed lines represent the Fermi level (shifted to 0 eV).

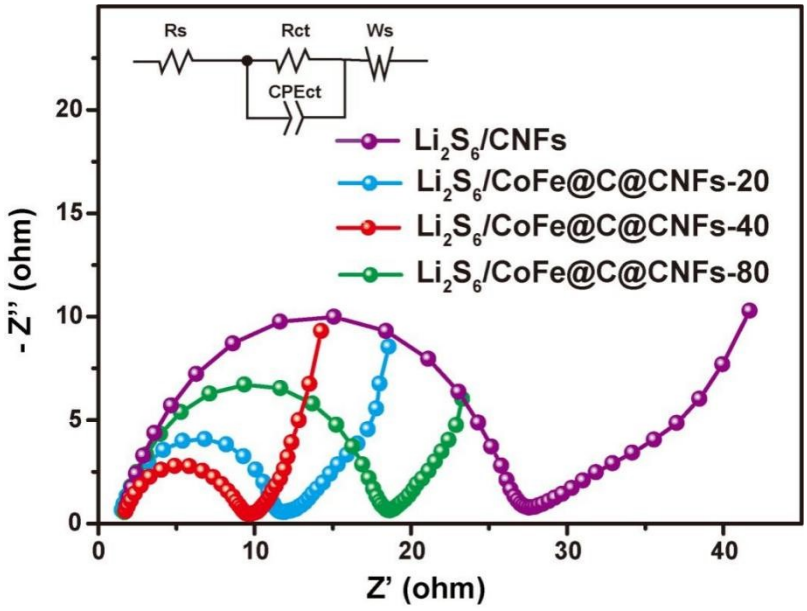

Fig. S8 EIS of Li-S batteries with different materials. Inset: the corresponding equivalent circuit model.

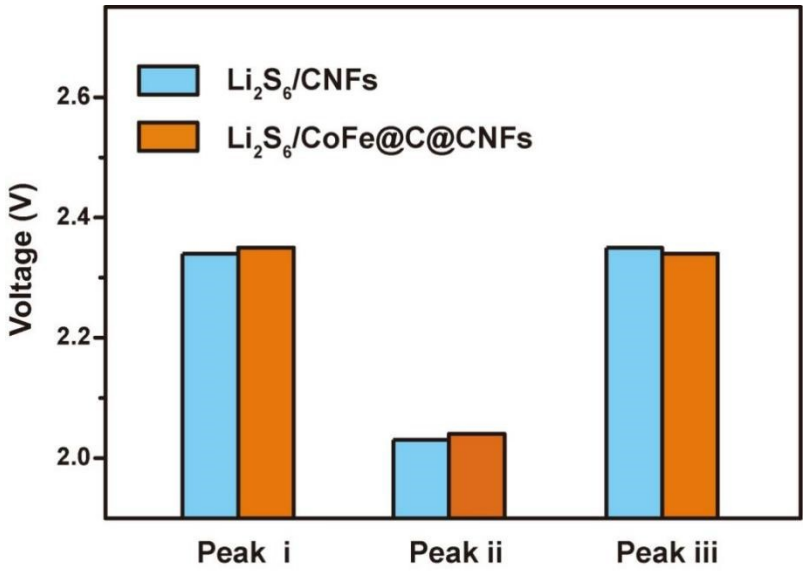

Fig. S9 Peak voltages of Li-S batteries using Li_2S_6/CNFs and Li_2S_6/CoFe@C@CNFs.

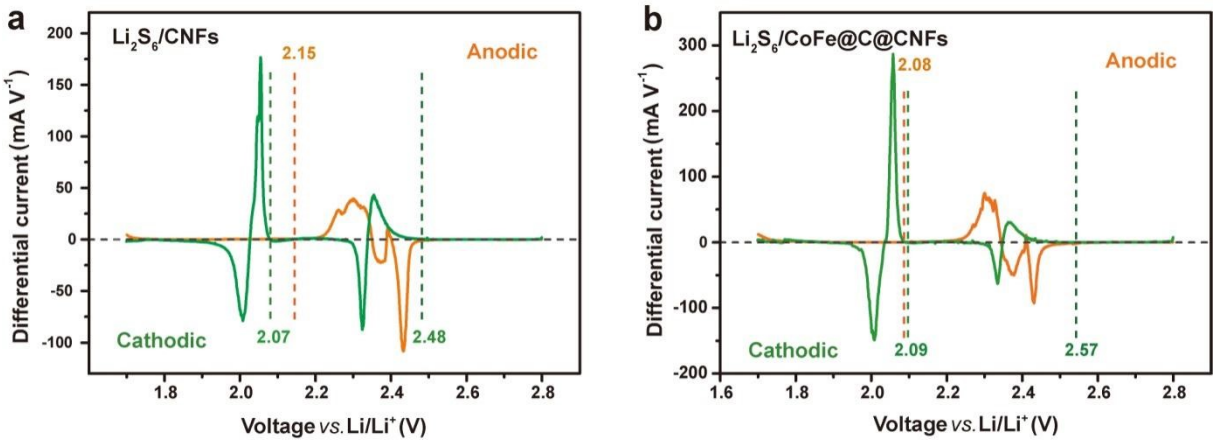

Fig. S10 Onset potentials of Li-S batteries using (a) Li_2S_6/CNFs and (b) Li_2S_6/CoFe@C@CNFs.

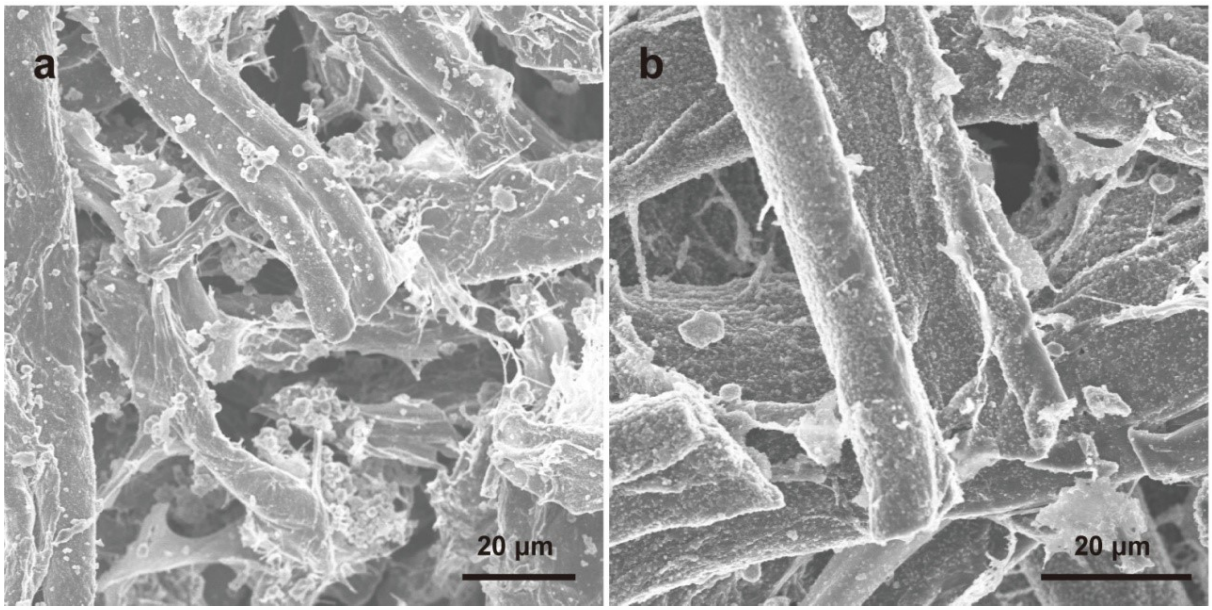

Fig. S11 Surface morphologies of (a) CNFs and (b) CoFe@C@CNFs after 300 cycles at 5 C.

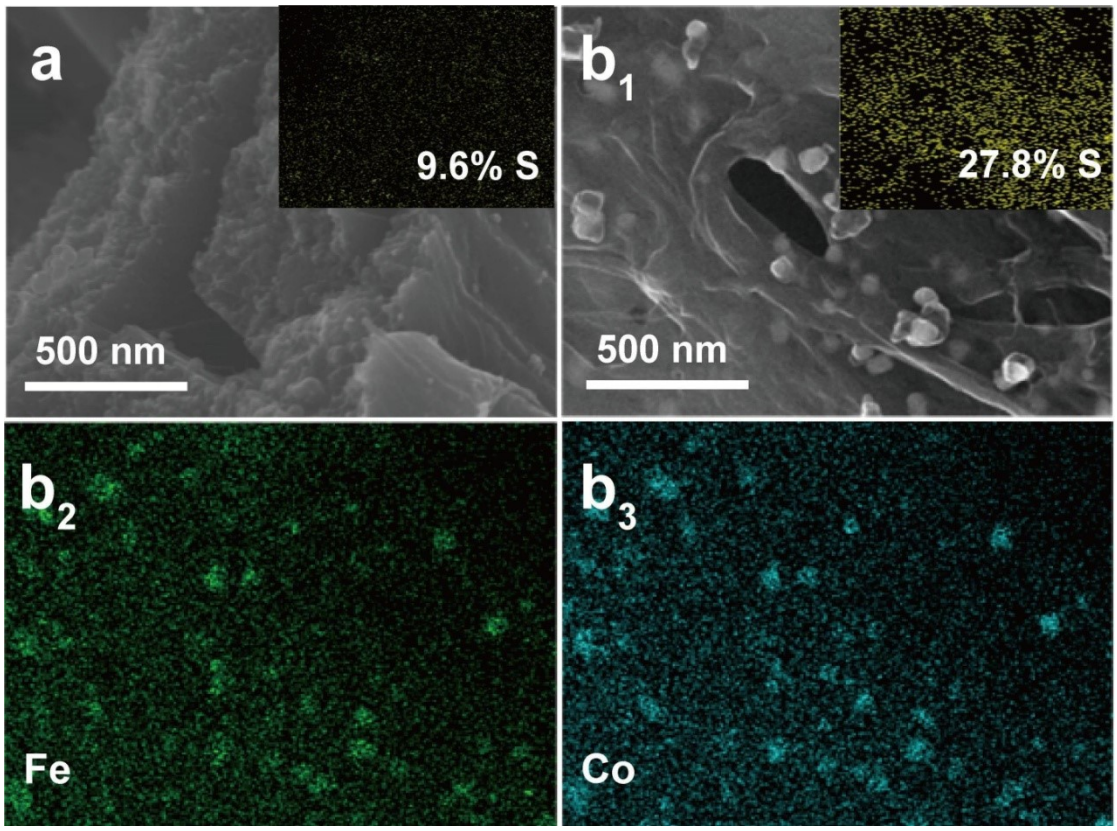

Fig. S12 (a) SEM image of CNFs after cycling. (b) SEM image and the corresponding elemental mapping images of CoFe@C@CNFs after cycling. Inset: S element mapping.

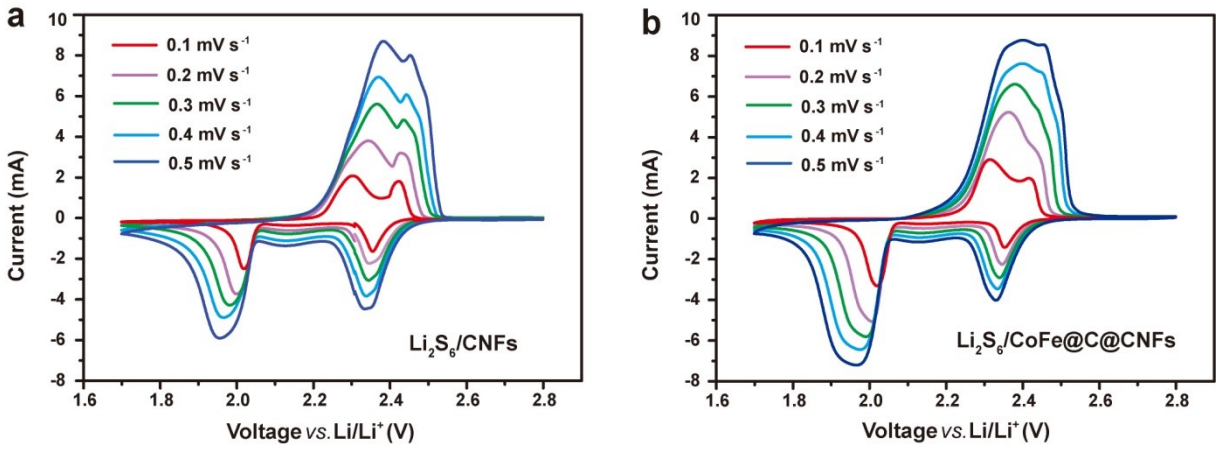

Fig. S13 CV curves at various voltage scan rates of Li-S batteries using (a) Li_2S_6/CNFs and (b) Li_2S_6/CoFe@C@CNFs.

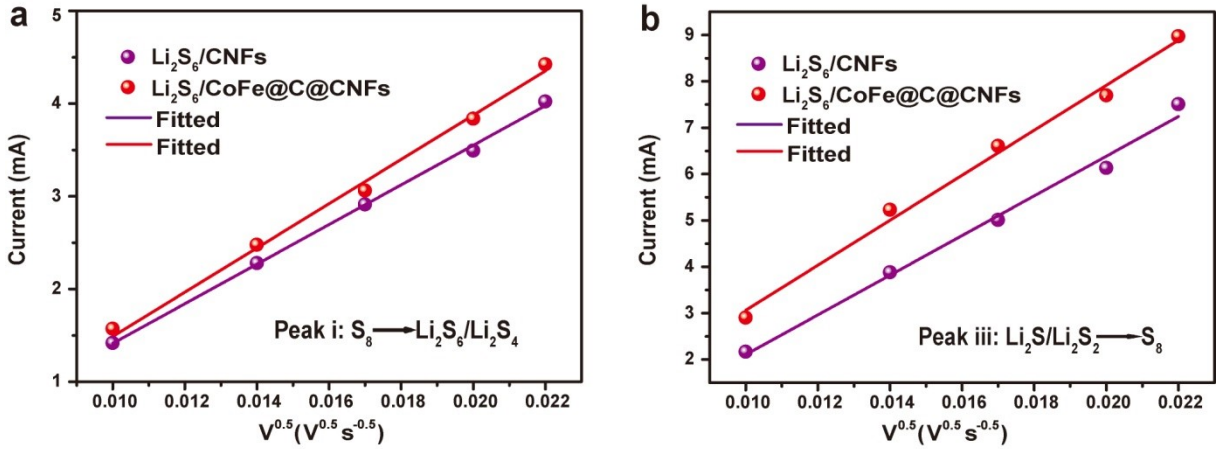

Fig. S14 Linear fits of the redox peak currents of Li-S batteries with Li_2S_6/CNFs and Li_2S_6/CoFe@C@CNFs at various voltage scan rates.

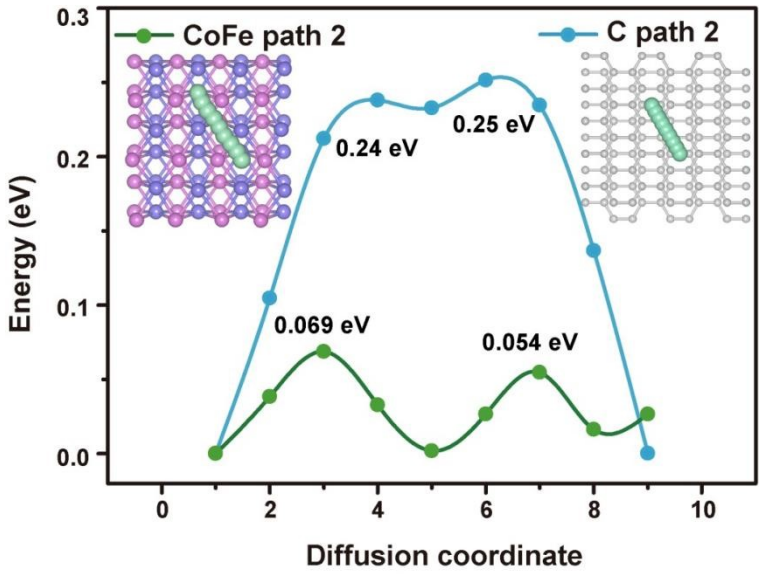

Fig. S15 Energy profile of lithium diffusion along path II for CoFe and CNFs. Inset: The corresponding schematic diagram of the top view of the considered migration paths for Li diffusion in CNFs and CoFe supercell.

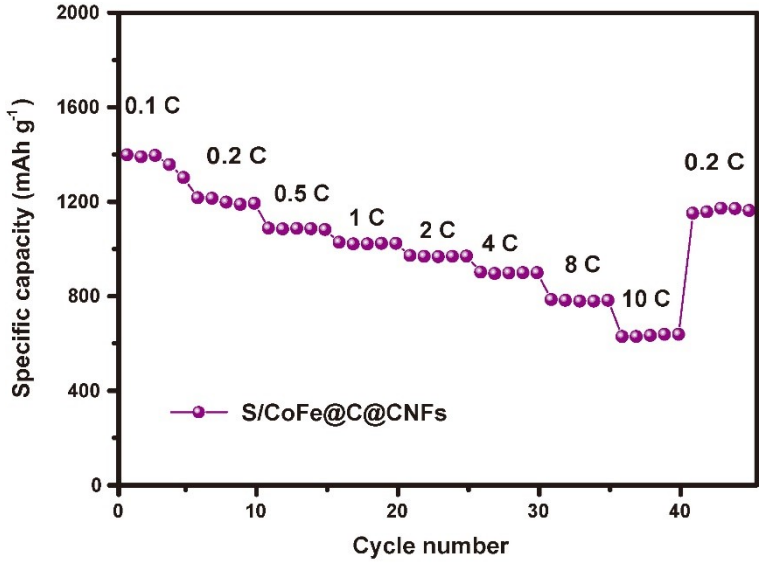

Fig. S16 Rate performances of Li-S batteries using S/CoFe@C@CNFs.

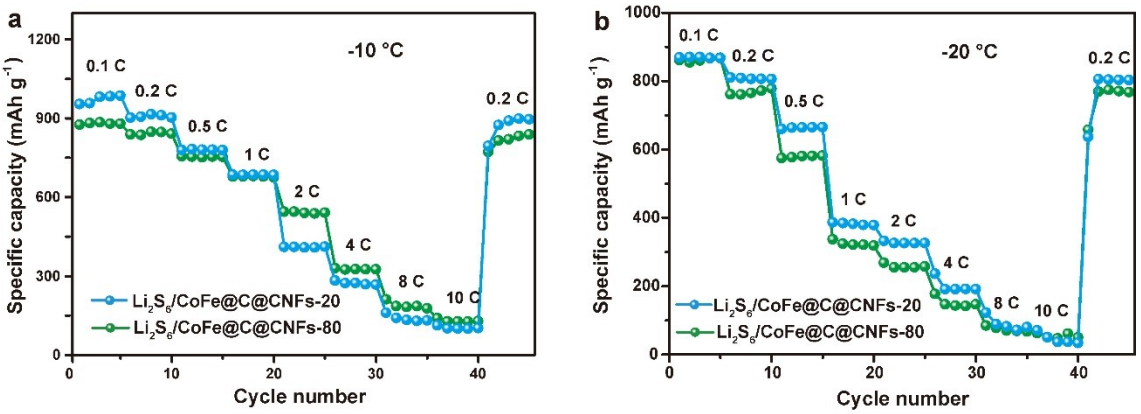

Fig. S17 Rate performances of Li-S batteries with different electrodes at (a) -10 °C and (b) -20 °C.

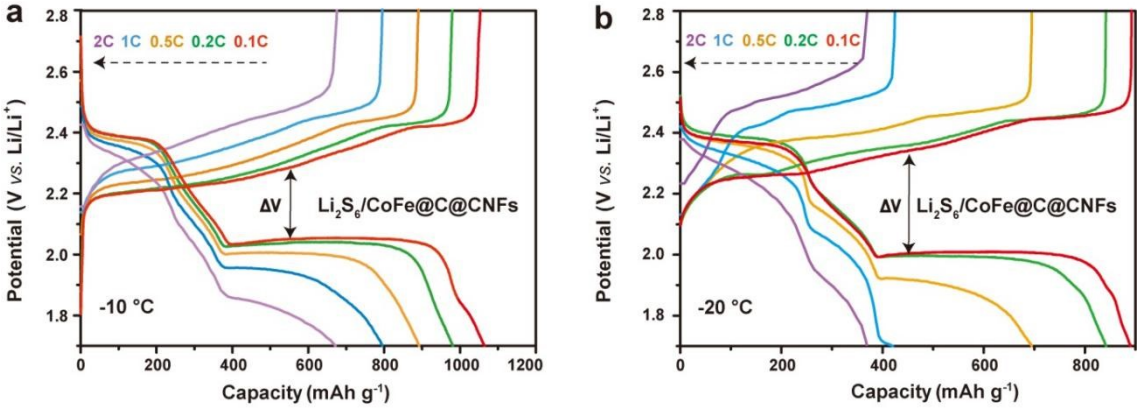

Fig. S18 Galvanostatic discharge/charge profiles of Li-S batteries with Li_2S_6/CoFe@C@CNFs at -10 °C and -20 °C.

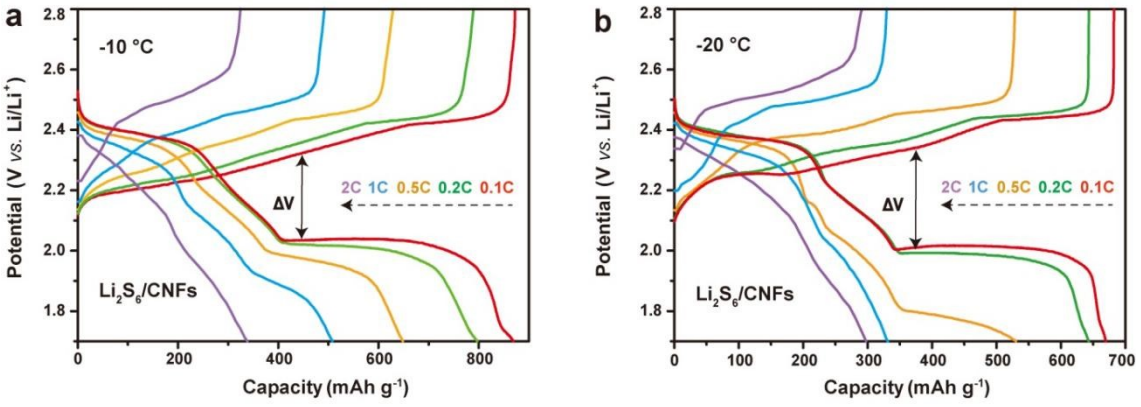

Fig. S19 Galvanostatic discharge/charge profiles of Li-S batteries with Li_2S_6/CNFs at -10 °C and -20 °C.

Table S1. The contents of the two metals in different materials.

Samples	Co	Fe
CoFe@C@CNFs-20	4.05%	3.84%
CoFe@C@CNFs-40	5.15%	4.89%
CoFe@C@CNFs-80	7.73%	7.33%

Table S2. Impedance parameters and electrical conductivity of different materials.

Samples	R_s (Ω)	R_{ct} (Ω)	Electrical Conductivity(S cm^{-1})
CNFs	1.8	25.7	1.08987768
CoFe@C@CNFs-20	1.5	10.5	2.62221549
CoFe@C@CNFs-40	1.7	7.85	1.79558391
CoFe@C@CNFs-80	1.7	16.9	1.30053076

Table S3. Performances comparison of this work with other cells using Li_2S_6 as the active substance.

Materials	0.1C (mAh g^{-1})	0.5C (mAh g^{-1})	2C (mAh g^{-1})	10C (mAh g^{-1})	Ref.
Li_2S_6/rGO	1607	1381	1194	—	[7]
Li_2S_6@SnS_2@N-CNFs	1137	809	—	—	[8]
Li_2S_6/CNF/rGO	—	623	581	—	[9]
WS_2- rGO-CNT/Li_2S_6	1270	1030	614	—	[10]
CSCNC@Li_2S_6	1377	1022	—	—	[11]
Mo_2C@CFs@Li_2S_6	1137	875	637	—	[12]
Li_2S_6/CoFe@C@CNFs	1655	1316	1197	828	This work

Table S4. Performances comparison of this work with other cells using elemental sulfur as the active substance.

Materials	0.2C (mAh g^{-1})	0.5C (mAh g^{-1})	2C (mAh g^{-1})	10C (mAh g^{-1})	Ref.
S@CoFe-MCS	1210	1050	750	—	[13]
S@CoFe/N-doped carbon	1275	1050	718	—	[14]
S/FeCo-C	1250.8	966.6	814.1	—	[15]
Fe/Co−N@C/S	1308	—	802	—	[16]
Fe/Co-C3N4/C/S	911	692	453	—	[17]
S/Co@N−C	1100	870	666	290	[18]
S/CoFe@C@CNFs	1215	1087	970	628	This work

Table S5. Performances comparison of this work with previous works at -20 °C.

Materials	0.1C (mAh g^{-1})	0.5C (mAh g^{-1})	2C (mAh g^{-1})	Ref.
nanocarbon/sulfur	755	360	234	[19]
BN/graphene	—	669	—	[20]
GO-Zn(II)-AmTZ/sulfur	620	354	—	[21]
Boron nitride nanosheet electrolyte	525	—	—	[22]
Nitrogen-Enriched Carbons/Sulfur	—	370	—	[23]
Li_2S_6/CoFe@C@CNFs	890	695	369	This work

Supplementary references

1 J. Hutter, M. Iannuzzi, F. Schiffmann, J. VandeVondele, *Wires. Comput. Mol. Sci.* **2014**, 4, 15.

2 T. D. Kuhne, M. Iannuzzi, M. Del Ben, V. V. Rybkin, P. Seewald, F. Stein, T. Laino, R. Z. Khaliullin, O. Schutt, F. Schiffmann, D. Golze, J. Wilhelm, S. Chulkov, M. H. Bani-Hashemian, V. Weber, U. Borstnik, M. Taillefumier, A. S. Jakobovits, A. Lazzaro, H. Pabst, T. Muller, R. Schade, M. Guidon, S. Andermatt, N. Holmberg, G. K. Schenter, A. Hehn, A. Bussy, F. Belleflamme, G. Tabacchi, A. Gloss, M. Lass, I. Bethune, C. J. Mundy, C. Plessl, M. Watkins, J. VandeVondele, M. Krack, J. Hutter, *J. Chem. Phys.* **2020**, 152, 194103.

3 John, P., Perdew, Kieron, Burke, Matthias, Ernzerhof, *Phys. Rev. Lett.* **1997**.

4 S. Goedecker, M. Teter, J. Hutter, *Phys. Rev. B: Condens. Matter.* **1995**, 54, 1703.

5 G. Henkelman, B. P. Uberuaga, H. Jonsson, *J. Chem. Phys.* **2000**, 113, 9901.

6 J. Shen, Z. Wang, X. Xu, Z. Liu, D. Zhang, F. Li, Y. Li, L. Zeng, J. Liu, *Adv. Energy Sustainability Res.* **2021**, 2, 2100007.

7 P. Chiochan, S. Kosasang, N. Ma, S. Duangdangchote, M. Sawangphruk, *Carbon* **2019**, 158.

8 S. S. Yao, C. J. Zhang, F. W. Xie, S. K. Xue, K. D. Gao, R. D. Guo, X. Q. Shen, T. B. Li, S. B. Qin, *Acs Sustain. Chem. Eng.* **2020**, 8, 2707.

9 S. C. Han, X. Pu, X. L. Li, M. M. Liu, M. Li, N. Feng, S. Dou, W. G. Hu, *Electrochim. Acta* **2017**, 241, 406.

10 S. Huang, Y. Wang, J. Hu, Y. V. Lim, D. Kong, Y. Zheng, M. Ding, M. E. Pam, H. Y. Yang, *ACS Nano* **2018**, 12, 9504.

11 S. S. Yao, C. J. Zhang, R. D. Guo, A. Majeed, Y. P. He, Y. Q. Wang, X. Q. Shen, T. B. Li, S. B. Qin, *Acs Sustainable Chem. Eng.* **2020**, 8, 13600.

12 Y. Y. Li, S. S. Yao, C. J. Zhang, Y. P. He, Y. Q. Wang, Y. Z. Liang, X. Q. Shen, T. B. Li, S. B. Qin, W. Wen, *Int. J. Energy Res.* **2020**, 44, 8388.

13 Z. Shi, Z. Sun, J. Cai, Z. Fan, J. Jin, M. Wang and J. Sun, *Adv. Func. Mater.* **2021**, 31, 2006798.

14 W. Qi, W. Wu, B. Cao, Y. Zhang and Y. Wu, *Inter. J. Hydrogen Energy* **2019**, 44, 20257-20266.

15 H. Li, L. Fei, R. Zhang, S. Yu, Y. Zhang, L. Shu, Y. Li and Y. Wang, *J. Energy Chem.* **2020**, 49, 339-347.

16 H. L. Ye, J. G. Sun, S. L. Zhang, H. B. Lin, T. R. Zhang, Q. F. Yao, J. Y. Lee, *ACS Nano* **2019**, 13, 14208-14216.

17 Y. F. Li, M. F. Chen, P. Zeng, H. Liu, H. Yu, Z. G. Luo, Y. Wang, B. B. Chang, X. Y. Wang, *J. Alloys Comp.* **2021**, 873, 159883.

18 Y. J. Li, J. M. Fan, J. H. Zhang, J. F. Yang, R. M. Yuan, J. K. Chang, M. S. Zheng, *ACS Nano* **2017**, 11, 11417-11424.

19 J. Q. Huang, X. F. Liu, Q. Zhang, C. M. Chen, M. Q. Zhao, S. M. Zhang, W. C. Zhu, W. Z. Qian, F. Wei, *Nano Energy* **2013**, 2, 314.

20 D. R. Deng, F. Xue, C. D. Bai, J. Lei, R. Yuan, M. S. Zheng, Q. F. Dong, *ACS Nano* **2018**, 12, 11120.

21 Z. Q. Zhang, Y. Q. Wang, J. Liu, D. Y. Sun, X. D. Ma, Y. C. Jin, Y. J. Cui, *Electrochim. Acta* **2018**, 271, 58.

22 J. Y. Wu, X. W. Li, Z. X. Rao, X. N. Xu, Z. X. Cheng, Y. Q. Liao, L. X. Yuan, X. L. Xie, Z. Li, Y. H. Huang, *Nano Energy* **2020**, 72, 104725.

23 S. Zhu, Y. Wang, J. Jiang, X. Yan, D. Sun, Y. Jin, C. Nan, H. Munakata, K. Kanamura, *ACS Appl. Mater. Interfaces* **2016**, 8, 17253.